

Effect of cleaning methods on the dissolution of diatom frustules

Emily M. Saad^a, Rebecca A. Pickering^b, Kanaha Shoji^a, Mohammad I. Hossain^c, T. Grant Glover^c, Jeffrey W. Krause^{b,d,*}, Yuanzhi Tang^a

^a School of Earth and Atmospheric Sciences, Georgia Institute of Technology, Atlanta, GA 30332, USA

^b Department of Marine Sciences, University of South Alabama, Mobile, AL 36688, USA

^c Department of Chemical and Biomolecular Engineering, University of South Alabama, Mobile, AL 36688, USA

^d Dauphin Island Sea Lab, Dauphin Island, AL 36528, USA

ARTICLE INFO

Keywords:

Diatoms
Biogenic silica
Thalassiosira
Dissolution
Sediment cleaning

ABSTRACT

Experimental studies characterizing the reactivity of siliceous materials, such as biogenic silica from the field or laboratory cultures, typically require organic matter removal prior to experimental analysis. Consequently, it is highly desired to develop and optimize a cleaning protocol that imposes minimal alterations to the reactivity of the siliceous substrate and can be robustly employed among laboratories and investigators. This study offers a quantitative comparison of several methods for removing organic matter associated with biogenic silica to assess their efficacy for use in reactivity studies. Five protocols for organic matter removal were assessed, including combinations of chemical treatments and/or baking, along with low temperature ashing with an oxygen plasma. These methods were tested and evaluated using *Thalassiosira pseudonana* frustules for mass recovery, organic carbon removal, elemental composition, morphology, structural order, relative abundance of silanol ($\equiv\text{Si}-\text{OH}$) groups, and dissolution rate. An additional experiment was conducted over a longer time scale using *Thalassiosira weissflogii* and a more realistic seawater matrix. Low temperature plasma ashing was found to be the most suitable for organic matter removal in studies seeking to constrain the short-term dissolution of biogenic silica; this method efficiently removed organic carbon while being the least impactful on frustule dissolution compared to the other cleaning methods evaluated. However, if the line of inquiry for an experiment does not require understanding of short-term dissolution rates, commonly used chemical (e.g. mineral acid, peroxide) and high temperature treatments did not appear to affect the long-term trajectory in biogenic silica dissolution.

1. Introduction

Amorphous silica is grossly undersaturated in seawater (Stumm and Morgan, 1996), and diatoms coat their siliceous cell walls with organic material to prevent their dissolution (Lewin, 1961). After diatom death, this organic material is subject to degradation by bacteria (Bidle and Azam, 1999), exposing the interior silica framework, and accelerating the rate of frustule dissolution (Kamatani et al., 1980). Because the dissolution of diatom silica (biogenic silica, bSiO_2) lags remineralization of its protective organic matter, bSiO_2 dissolution can be a first-order metric for diagnosing the reduction of diatoms contribution to the biological carbon-dioxide pump in the water column and their capacity to sequester organic matter into the geological carbon cycle in sediments (Laruelle et al., 2009). Most pelagic diatom productivity is remineralized in the water column as only $\sim 10\%$ of the bSiO_2 produced in the photic zone reaches the seabed (Trégouer and De La Rocha, 2013). In the open ocean, 88–95% of this bSiO_2 delivered to the sediments

dissolves, and this trend largely holds even in high bSiO_2 sediments (e.g. Southern Ocean, 91–98%; except for the inner Ross Sea 42%—annual averaged values from review by Trégouer and De La Rocha (2013)). These data demonstrate that in a vast majority of the oceanic area, and in most vertical layers, dissolution of bSiO_2 is the dominant silicon (Si) cycle rate process. To understand the transport of bSiO_2 through the water column and its fate in the sediments, marine sedimentary processes involving bSiO_2 must be better constrained (DeMaster, 2003). While the dissolution kinetics of bSiO_2 in sediments has been the subject of much study for over 50 years (e.g. Dixit and Van Cappellen, 2002; Hurd and Birdwhistell, 1983; Lewin, 1961; McManus et al., 1995), new information on the significance of various marine sediment Si-cycle processes such as marine secondary clay formation (Michalopoulos and Aller, 1995; Michalopoulos et al., 2000; Rahman et al., 2017) necessitates the need to standardize how we study it in laboratory experiments.

Transformation of bSiO_2 in the sediments initiates with the

* Corresponding author at: Department of Marine Sciences, University of South Alabama, Mobile, AL 36688, USA.
E-mail address: jkrause@disl.edu (J.W. Krause).

dissolution of diatom cell walls, thus, an operational issue for laboratory studies is removing the organic coating surrounding bSiO_2 in a manner consistent with natural conditions (e.g. bacterial degradation of the organic matrix). The multi-faceted challenge for any cleaning procedure is to be efficient, repeatable, and not significantly alter the bSiO_2 surface. It is well established that bSiO_2 surface structure is strongly correlated to its chemical reactivity (Loucaides et al., 2010a and references therein). Once exposed, the dissolution kinetics of bSiO_2 are intimately linked to the chemical structure at the solid-solution interface (e.g. Van Cappellen et al., 2002), such as the concentration, distribution, and composition of surface silanol groups ($\equiv\text{Si}-\text{OH}$), siloxane groups ($\text{Si}-\text{O}-\text{Si}$), and the porous structure of the silica (Zhuravlev, 2000). Furthermore, as evidenced by the formation of surface precipitates on diatoms during early diagenesis (Michalopoulos et al., 2000), the integrity of the surface structure of the bSiO_2 must be maintained during the organic matter removal process.

Previous comparisons of frustule cleaning methods were primarily limited to microscopic and composition characterizations, such as stable isotope and element ratio (Blanco et al., 2008; Morales et al., 2013; Tyler et al., 2007; Xiong et al., 2012). A recent study quantitatively compared and assessed several cleaning methods for the isotopic determination of diatom frustule-bound nitrogen for the potential application of this system as a paleo proxy for marine productivity (Morales et al., 2013). With the recent interests in material and nanotechnological applications of diatom-derived bSiO_2 (Jeffries et al., 2011; Losic et al., 2009), a few laboratory studies have quantitatively compared frustule pore size, surface area, and composition under several cleaning conditions (e.g. Van Eynde et al., 2014). When trying to understand postmortem dissolution, some researchers have opted not to treat diatom material artificially, instead using natural bacterial assemblages to strip organic matter (Boutorh et al., 2016). While this approach is elegant and best simulates environmental conditions, it is difficult to be repeatable among laboratories due to dependence on factors such as the initial bacterial community composition, biomass, activity, and incubation temperature (Bidle et al., 2003).

The most frequently employed cleaning methods are high temperature baking, hydrogen peroxide, mineral acids, and sodium dodecyl sulfate (SDS)/ethylenediaminetetraacetic acid (EDTA) treatments (Boyle et al., 1984; Dean, 1974; Tesson et al., 2008; Van der Werff, 1955). Intense treatments, such as nitric acid and hydrogen peroxide, have been used to strip organic matter to infer Si dissolution and associated isotopic fractionation (Demarest et al., 2009), but these chemicals are thought to cause selective etching of the frustule surface; whereas gentle methods may not effectively remove sufficient organic matter (Van Eynde et al., 2014). Acid-cleaned bSiO_2 commonly exhibits a more rapid dissolution rate than those from natural siliceous assemblages of phytoplankton (Lawson et al., 1978). However, systematic characterization and comparison of reactivity alterations after different cleaning treatments are still limited.

Any organic removal method for diatom bSiO_2 must keep in mind the ultimate utility for the material. For use in reactivity studies, the ideal cleaning method will remove organic matter and loosely adsorbed cations while not significantly affecting the structure, phase (e.g. thermal annealing pushes SiO_2 toward more ordered phases like cristobalite), and reactivity. Among all available methods for preparing diatom frustules for reactivity tests, one promising method is low temperature plasma ashing (Koning et al., 2007; Loucaides et al., 2010b). This method was originally proposed as a gentle and efficient method for removing organic matter of diatom species with delicate frustule structures for taxonomic identification (Watanabe et al., 2010). However, no quantitative assessments are currently available on this cleaning process and resulting frustule composition, structure, and reactivity. In this study, we treated the diatom *Thalassiosira pseudonana* (*T. pseudonana*) using several representative cleaning methods to purify its bSiO_2 , and the treated materials were reacted under controlled laboratory conditions. Morphology, structure, and dissolution of the

materials from different treated methods were systematically characterized and compared to quantitatively assess the method suitability for bSiO_2 reactivity studies using dissolution as a proxy for reactivity. We then examined longer-term dissolution trends, but in fewer treatments, using a more complex and realistic model system, specifically using natural seawater with *Thalassiosira weissflogii* (*T. weissflogii*), which is a larger species than the *T. pseudonana* but has similar shape and structure.

2. Materials and procedures

2.1. Short-term controlled laboratory experiments in artificial seawater

2.1.1. Biomass cleaning

Both *T. pseudonana* and *T. weissflogii* were procured from Reed Mariculture Inc. The raw algal paste (i.e. without any proprietary additives or preservatives) was stored at $-20\text{ }^\circ\text{C}$ until used in the laboratory. All cleaning procedures using different methods were performed within the same week. Prior to use, biomass was thawed and repeatedly rinsed with deionized water (DI, $18\text{ M}\Omega\text{ cm}$) to remove residual growth media. Rinsing involved suspending $\sim 1\text{ g}$ of wet biomass in 50 mL of DI, followed by repeated shaking and centrifugation ($2.2 \times 10^3\text{ g}$, 5 min) until the conductivity of the supernatant was constant and similar to deionized water ($< 20\text{ }\mu\text{S cm}^{-1}$). This rinsed material was then freeze-dried (hereafter referred to as raw material) and gently disaggregated for organic matter removal by a survey of commonly employed methods (Table 1). The evaluated methods included hydrochloric acid and high temperature baking (HCl + baking), high temperature baking only (baking only), heated hydrogen peroxide (H_2O_2), heated nitric acid (HNO_3), hydrogen peroxide and heated HCl ($\text{H}_2\text{O}_2 + \text{HCl}$), and low temperature plasma ashing (LTP). All techniques have been used previously in separate studies (Abramson et al., 2009; Jiang et al., 2014; Watanabe et al., 2010). Each treatment was performed in duplicate. After each treatment, solid samples were repeatedly centrifuged, aspirated, and rinsed in DI water until the conductivity of the supernatant was similar to DI ($< 20\text{ }\mu\text{S cm}^{-1}$), then freeze dried for subsequent characterizations. A portion of the raw material was also preserved for subsequent analyses.

2.1.2. Characterization of the raw and cleaned materials

Raw and cleaned materials were characterized for composition, morphology, and structural properties. Organic carbon content was measured by combustion using a CHNSO analyzer (Costech Instruments) after acid fuming over night (Hedges and Stern, 1984). A portion of the solids were also digested using 0.2 M NaOH for 15 min at $100\text{ }^\circ\text{C}$ (Krausse et al., 1983) and analyzed for magnesium (Mg), potassium (K), calcium (Ca), aluminum (Al), and iron (Fe) concentrations using inductively coupled plasma-mass spectrometry (ICP-MS, Agilent 7500a). A separate subsample of this digested material was analyzed for dissolved silicic acid concentration ($[\text{Si}(\text{OH})_4]$, representative of solubilized bSiO_2) following the molybdenum blue method (Strickland and Parsons, 1972) using an UV-vis spectrophotometer (Agilent Cary 60). A Micromeritics 3Flex porosimeter was used to measure the N_2 adsorption isotherms at $-196.15\text{ }^\circ\text{C}$, and the surface area of the solids was calculated using the Brunauer–Emmett–Teller (BET) N_2 sorption method. The surface area data was collected using a $100\text{ }^\circ\text{C}$ regeneration temperature. The motivation for the selection of this temperature, and the details necessary to reproduce these measurements (see Supporting Information, SI; Figs. S1, S2), are provided because such information is typically unreported in the literature when making similar measurements on diatom bSiO_2 . Morphology of the solid was characterized using scanning electron microscopy (SEM; Hitachi SU-8230). Solid structure was characterized using X-ray diffraction (XRD, PANalytical Empyrean, $\text{Cu K}\alpha$ source). Order and relative abundance of silanol and siloxane groups was characterized using Attenuated Total Reflection–Fourier Transformed Infrared (ATR-FTIR) spectroscopy

Table 1

Summary of the organic matter removal techniques compared in this study.

Treatment	Method Description	Reference
HCl + baking	<ul style="list-style-type: none"> 1 g (dry weight) of biomass suspended in 50 mL of 15% hydrochloric acid (HCl, trace metal grade, Sigma-Aldrich) in a 500 mL beaker, boiled for 1 h while continuously stirring, allowed to cool Transferred to a 50 mL centrifuge tube, repeatedly rinsed by centrifugation and resuspension in DI until the pH of the supernatant was like that of DI (~ 6) Supernatant was decanted, and solid was dried at 120 °C until completely dry Heated in a furnace at 600 °C for 6 h 	Jiang et al., 2014
Baking	<ul style="list-style-type: none"> 1 g (dry weight) evenly spread into a thin layer in 500 mL beaker Heated in a furnace at 600 °C for 6 h 	Jiang et al., 2014
Low temperature plasma ashing (LTP)	<ul style="list-style-type: none"> 0.2 g material placed in glass petri dishes and treated by low temperature plasma ashing (Plasma-Therm RIE) at 350 W, 25 °C, O₂ flow rate = 60 sccm for 7 h) 	Watanabe et al., 2010
H ₂ O ₂	<ul style="list-style-type: none"> 0.5 g (dry weight) suspended in 50 mL of 15% hydrogen peroxide (H₂O₂, trace metal grade, Sigma-Aldrich), heated at 60 °C for 48 h in a 500 mL beaker Transferred to a 50 mL centrifuge tube, repeatedly rinsed by centrifugation and resuspension in DI until the pH of the supernatant was similar to the pH of DI (~ 6) 	Van Eynde et al., 2014
HNO ₃	<ul style="list-style-type: none"> 1 g (dry weight) suspended in 50 mL of 30% nitric acid (HNO₃, trace metal grade, Sigma-Aldrich) in a 500 mL beaker, heated at 60 °C for 48 h Transferred to a 50 mL centrifuge tube, repeatedly rinsed by centrifugation and resuspension in DI until the pH of the supernatant was similar to the pH of DI (~ 6) 0.5 g (dry weight) suspended in 50 mL of 30% H₂O₂ overnight Transferred to a 50 mL centrifuge tube, repeatedly rinsed by centrifugation and resuspension in DI until the pH of the supernatant was similar to the pH of DI (~ 6) Resuspended in 6 M HCl at 110 °C for 20 h Transferred to a 50 mL centrifuge tube, repeatedly rinsed by centrifugation and resuspension in DI until the pH of the supernatant was similar to the pH of DI (~ 6) 	Van Eynde et al., 2014
H ₂ O ₂ + HCl		Abramson et al., 2009

(Bruker Equinox 55).

2.1.3. Dissolution of cleaned material

The short-term dissolution rate and extent (i.e. total [Si(OH)₄]) for cleaned *T. pseudonana* was characterized in controlled laboratory conditions by incubating cleaned bSiO₂ with artificial seawater under sterile conditions for ~1 month in the dark at room temperature. Cleaned and UV-sterilized (to remove bacteria) *T. pseudonana* biomass from each duplicate treatment (0.1 g L⁻¹) were suspended in 100 mL of filter sterilized (0.2 µm, cellulose acetate) artificial seawater (Kester et al., 1967) buffered with 15 mM 4-(2-hydroxyethyl)-1-piperazineethanesulfonic acid (HEPES, high purity grade) at pH 7 in polypropylene bottles. Cleaning treatments affected the ratio of bSiO₂ to total sample mass (Table 2). Suspensions were constantly agitated on a shaker table. 200 µL aliquots of each sample were collected over time, syringe filtered (0.2 µm, PTFE, VWR), and analyzed for [Si(OH)₄] using the same method discussed above. pH was also monitored at each time point and readjusted to 7.0 ± 0.1 as the samples tended toward 7.3 ± 0.1 during dissolution. No microbial growth was visually observed (e.g. biofilm, floc) throughout the experiments. Replicates of one sample from each treatment were also conducted, and the error associated with the dissolution experiment alone was significantly less than that of the duplicates of each treatment. The presented errors associated with each average are a result of the propagation of error associated with duplicate cleaning methods as with duplicate dissolution experiments.

Table 2Characteristics of raw and cleaned *T. pseudonana*. Error is ± standard deviation.

Treatment	Mass Recovery (%)	Organic Carbon Content (wt%)	Fe Content (wt%)	BET surface area at 100 °C (m ² g ⁻¹)	bSiO ₂ content in cleaned material (mmol Si g ⁻¹)
HCl + baking	27 ± 3	0.07 ± 0.03	BDL	34	17.0 ± 1.9
Baking	38 ± 3	0.08 ± 0.01	1.4 ± 0.5	30	13.5 ± 1.6
LTP	34 ± 0.5	1.0 ± 0.09	0.4 ± 0.1	53	6.8 ^a
Raw	–	28.9 ± 0.4	0.7 ± 0.1	9	8.8 ± 2.0
H ₂ O ₂	26 ± 3	1.1 ± 0.07	0.4 ± 0.2	28	12.7 ± 1.2
HNO ₃	37 ± 0.3	2.2 ± 0.42	BDL	28	16.1 ± 2.3
H ₂ O ₂ + HCl	32 ± 6	10.1 ± 0.60	BDL	21	13.0 ± 0.9

Note: BDL (below detection limit of 0.13 wt%).

^a Insufficient material remained, therefore, no replicate but this is within one standard deviation of the raw material.

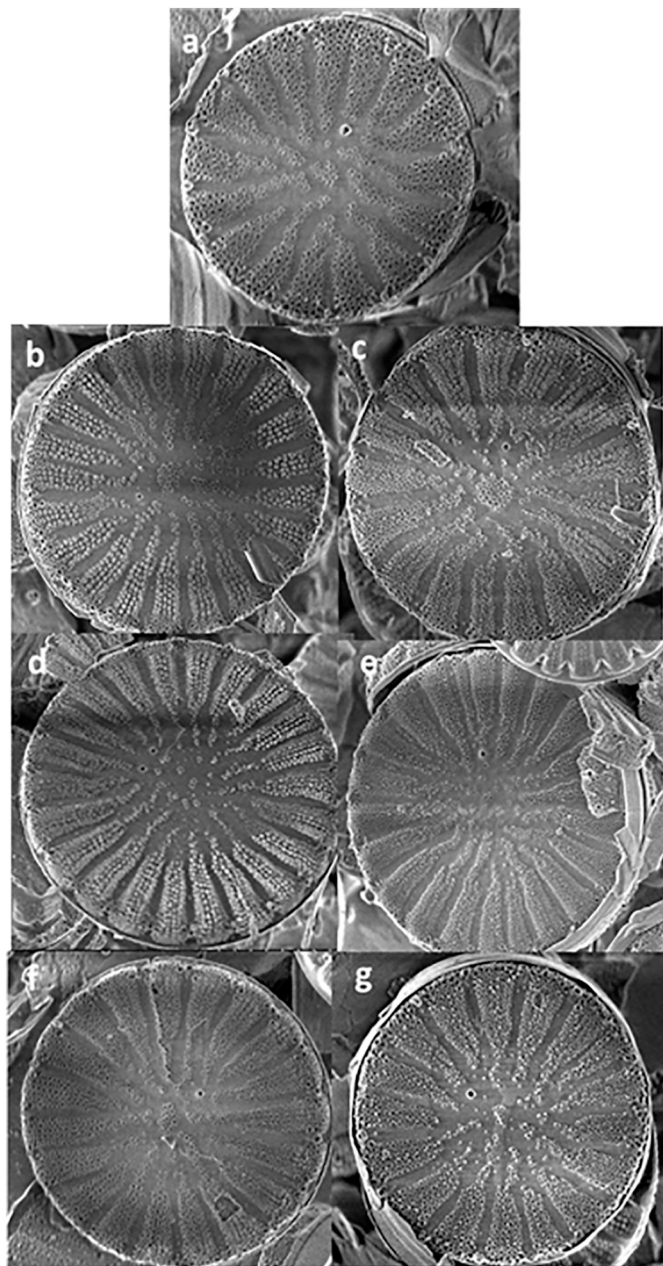


Fig. 1. Representative SEM images of *T. pseudonana* frustules (A) before cleaning (Raw) and after (B) HCl + baking, (C) baking only, (D) H₂O₂, (E) HNO₃, (F) H₂O₂ + HCl, (G) LTP treatments.

presentation of 28-day normalized rates (longest shared-time point) allows for the similarity in the temporal trends and their respective offsets between cleaning treatments to be highlighted. For comparison of initial dissolution behavior with the short-term experiments, the rate of increase (i.e. linear slope of the normalized released SiO₂, hence units of inverse time) during the first seven days was calculated, as this time period in both experiments showed parabolic kinetics among both species and treatments (discussed below).

3. Results and discussion

3.1. Characterization of biogenic silica cleaned by different methods

Parameters used for comparing different treatment methods include mass recovery, organic carbon content, concentrations of other elements, morphological alteration, structural alteration, and bSiO₂

dissolution. These parameters were quantitatively compared for *T. pseudonana* biomass cleaned under different conditions (Table 1).

Mass recovery was used as an indicator of method efficiency. Biogenic silica mass can be limited for natural samples, especially in low bSiO₂ content sediments (< 2% by mass, Krause et al., 2017), and significant losses in sample quantity might affect data interpretation (Watanabe et al., 2010; Xiong et al., 2012). Mass recovery can assess efficiency in terms of operator error (e.g. mass loss during transfer) as well as mass loss due to dissolution of solids during the cleaning process (Watanabe et al., 2010). The organic carbon content of the raw material was 28.1 ± 0.9 wt% (Table 2); thus, mass recovery less than ~70% can be attributed to mass loss due to sample handling and loss of material other than organic matter during cleaning process. The total range in mass recovery was 12%. The highest mass recoveries resulted from baking, LTP, and HNO₃ treatments (> 30% recovery) and the lowest from HCl + baking and H₂O₂ treatments (< 30%). In addition, the precision of the treatments can provide some insights into the robustness of the method. The methods resulting in the lowest percent relative standard deviation (RSD) were the LTP and HNO₃ treatments (1% RSD), followed by HCl + baking, baking only, and H₂O₂ treatments (8–10%), followed finally by H₂O₂ + HCl treatment (20%).

Elemental content was used to evaluate method efficacy. Of the recovered cleaned material, the lowest organic carbon content resulted from both baking treatments (< 0.1%), followed by LTP and H₂O₂ (~1%), HNO₃ (2.2%), and H₂O₂ + HCl treatment (10%). Mg, Ca, K, and Al were not found to be associated with the raw or cleaned material after the initial DI rinsing (detection limit in wt% for Mg, Ca, and K: ~1%; Al: ~0.1%). However, Fe was detected in the initial material and remained present in the materials cleaned by methods that did not involve acid (Table 2). It is likely that the Fe came from the growth medium and/or was associated within the frustule structure as Fe has been previously shown to incorporate into *T. pseudonana* diatom frustules during growth (Ellwood and Hunter, 2000), and reduced iron inside frustules has also been observed for diatoms in the Southern Ocean (Ingall et al., 2013).

Surface area analysis helped determine whether each method degraded the fine structure of the frustule. Several factors can affect the surface area, including organic matter content and potential alteration (e.g. break down) of the frustule material. The lowest BET specific surface area was observed in the raw material (9 m² g⁻¹), with the highest in the LTP treatment (53 m² g⁻¹) (Table 2). For all other treatments (excluding LTP), surface area and organic matter content were negatively correlated (Fig. S3, R² = 0.93, p < .01). Because the BET surface area analysis is dependent on the adsorption of N₂ gas molecules, the diatom bSiO₂ porosity and pore connectivity of samples are important influencing factors. Therefore, the significantly enhanced surface area of LTP treatment is possibly due to better removal of organic matter in pores and channels due to increased diffusion of gas molecules during LTP treatment than the aqueous solutions used in other treatments.

Solid phase characterizations were also performed to assess the potential alteration of diatom frustules by different cleaning methods. SEM analyses revealed no difference in morphology at the micrometer scale by different cleaning methods (Fig. 1). Random fragmentation was observed in samples from each treatment, most likely due to the repeated rinsing both before and after cleaning; however, this is common and also reflects breakage and fragmentation seen in bSiO₂ detritus (i.e. non-living diatoms), which can be the majority of total bSiO₂ (i.e. living diatoms + detritus) in field conditions (Krause et al., 2010), due to mechanical damage from herbivore grazing. XRD analysis revealed that after treatment, all materials were characterized as amorphous SiO₂ (i.e. opal-A), as evidenced by the presence of only a broad peak at 20–26° 20 (Fig. 2) (DeMaster, 2003). However, the peak shape changed among treatments (Fig. 2). The coefficient of variation (%cv) (i.e. standard deviation normalized to mean intensity) within the 20–26° 20 range was similar for the raw material (%cv = 17%) and the

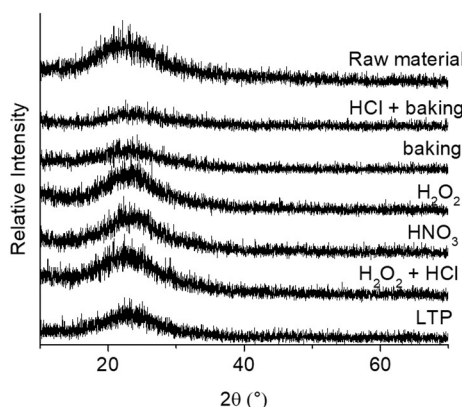


Fig. 2. XRD patterns of biogenic silica of *T. pseudonana* before and after cleaning, all in amorphous silica phases as indicated by the broad peak at $\sim 15\text{--}30^\circ$ 2θ .

$\text{H}_2\text{O}_2 + \text{HCl}$, HNO_3 , and H_2O_2 treatments (16–17%), whereas the %cv increased in the LTP (21%), baking (22%), and HCl + baking treatments (24%). None of the treatments, even baking, radically modified the bSiO_2 toward the formation of more ordered crystalline structures such as cristobalite.

FTIR was used to elucidate the relative abundances of silanol ($=\text{Si}-\text{OH}$) and siloxane ($\text{Si}-\text{O}-\text{Si}$) groups, as well as overall structural order (Zhuravlev, 2000). FTIR revealed the three vibration bands within the scan range that are indicative of amorphous silica (Fig. 3) (Iler, 1979; Legrand, 1998). The vibration bands at ~ 1100 , ~ 950 , and $\sim 800 \text{ cm}^{-1}$ wavenumbers can be attributed to the stretching vibration mode of the SiO_4 tetrahedron, the Si–O stretching of the $=\text{Si}-\text{OH}$ groups, and the bending vibration of inter-tetrahedral Si–O–Si bonds, respectively (Iler, 1979; Legrand, 1998). Ratios of the integrated absorption intensities at these energies can be used to elucidate the structural and molecular characterization of the solid (Table 3). The ratio of the integrated intensities of the 800 and 1100 cm^{-1} absorption bands (A_{800}/A_{1100}) has been used to indicate the three dimensional organization (degree of structure order) of the SiO_2 framework (Gendron-Badou et al., 2003), with increasing value associated with increasing structural order. The ratio of the integrated intensities of the 950 and 800 cm^{-1} absorption bands (A_{950}/A_{800}) was previously used to indicate the relative abundance of silanol group ($=\text{Si}-\text{OH}$) (Schmidt et al., 2001). The A_{800}/A_{1100} ratio was lowest for the raw material and LTP treatment (0.03), followed by H_2O_2 (0.05), then HCl + baking, HNO_3 , and $\text{H}_2\text{O}_2 + \text{HCl}$ treatments (0.06), and finally by the baking only treatment (0.07). The

Table 3

Peak characteristics (maximum divided by standard deviation) in XRD spectra intensity mean normalized to standard deviation among $20\text{--}26^\circ$ 2θ range (Fig. 2) and band intensity ratios for the FTIR spectra (Fig. 3, A_{800}/A_{1100} , A_{800}/A_{950}) for raw and cleaned *T. pseudonana*.

Treatment	$20\text{--}26^\circ$ 2θ %CV	A_{800}/A_{1100}	A_{950}/A_{800}
HCl + baking	23.5	0.06 ± 0.01	0.00 ± 0.00
Baking	22.3	0.07 ± 0.01	0.08 ± 0.06
LTP	21.3	0.03 ± 0.01	1.50 ± 0.16
Raw material	17.4	0.03 ± 0.01	1.70 ± 0.21
H_2O_2	17.0	0.05 ± 0.01	1.18 ± 0.05
HNO_3	16.4	0.06 ± 0.01	1.47 ± 0.09
$\text{H}_2\text{O}_2 + \text{HCl}$	15.9	0.06 ± 0.01	1.14 ± 0.05

A_{950}/A_{800} ratio for the raw material and LTP was the same as that reported previously for fresh *Thalassiosira punctigera* and *Cyclotella meneghiniana* (Loucaides et al., 2010a). The A_{950}/A_{800} ratio decreased from that of the raw material (1.70), to LTP (1.50), HNO_3 (1.47), H_2O_2 (1.18), $\text{H}_2\text{O}_2 + \text{HCl}$ (1.14), baking only (0.08), and finally HCl + baking (0) (Table 3).

3.2. Short-term dissolution of *T. pseudonana* in artificial seawater

The dissolution behavior of cleaned materials appeared to vary greatly (Fig. 4A). After ~ 30 days, HNO_3 treatment reached the greatest extent of dissolved SiO_2 ($\sim 1600 \mu\text{M}$), followed by $\text{H}_2\text{O}_2 + \text{HCl}$ ($\sim 1400 \mu\text{M}$), H_2O_2 and HCl + baking ($\sim 1100 \mu\text{M}$), baking only ($\sim 800 \mu\text{M}$), LTP ($\sim 600 \mu\text{M}$), and the raw material ($\sim 400 \mu\text{M}$). When adjusting for both the initial surface area and the bSiO_2 content per gram in the cleaned material (Table 2), dissolution in four treatments (HCl + baking, baking only, LTP, raw; Fig. 4B) obeyed parabolic kinetics (Greenwood et al., 2001 and references therein). Whereas H_2O_2 , HNO_3 , and $\text{H}_2\text{O}_2 + \text{HCl}$ treatments adhered to parabolic kinetics for ~ 168 h (7 days), consistent with the issue of truncation when using this model (Greenwood et al., 2001 and references therein), and then the surface-area normalized rate stabilized (Fig. 4C). Except for the LTP and raw material, the regression slopes (rate constant, units $10^{-10} \text{ mol cm}^{-2} \text{ h}^{-0.5}$) for the parabolic kinetic model are approximately an order of magnitude higher than reported for Antarctic diatom oozes dissolved between 15 and 25 °C (Fig. 4B, C; Kamatani et al., 1988). Such a result is not surprising given the diatoms used here were grown in culture and had not been preserved in the sediments. However, when converting the rate constant for our cleaning treatments to units expressed by other studies (e.g. $10^{-11} \text{ mol m}^{-2} \text{ s}^{-1}$; Dixit and Van Cappellen, 2002; Van Cappellen et al., 2002) the treatments range from 0.8 (LTP) to 16.4 ($\text{H}_2\text{O}_2 + \text{HCl}$). These previous studies reported a range of 0.2–14.0 for diatom cultures dissolved at lower temperatures (3 °C), which included two other species from the genus *Thalassiosira* (Van Cappellen et al., 2002). Given the Q_{10} change for bSiO_2 dissolution averages ~ 2.4 (Demarest et al., 2011), correcting for temperature differences increases the range reported by Van Cappellen et al. (2002), i.e. 0.7 to 52.1. All our treatments fall within this span, demonstrating our dissolution rates are consistent with previous studies. However, the raw material appeared to have much more dissolution per unit surface area than the cleaned materials, which emphasizes that caution must be used when applying laboratory-based rates on chemically treated diatom frustules to field conditions.

3.3. Long-term dissolution of *T. weissflogii* in natural seawater

The long-term dissolution of *T. weissflogii*, which had organic matter removed either by LTP or HNO_3 , was also used to probe the influence of cleaning method on the dissolution of bSiO_2 in a natural seawater matrix. Within the initial ~ 30 days, the LTP treatment resulted in both lower initial dissolution rate and extent compared to HNO_3 treatment

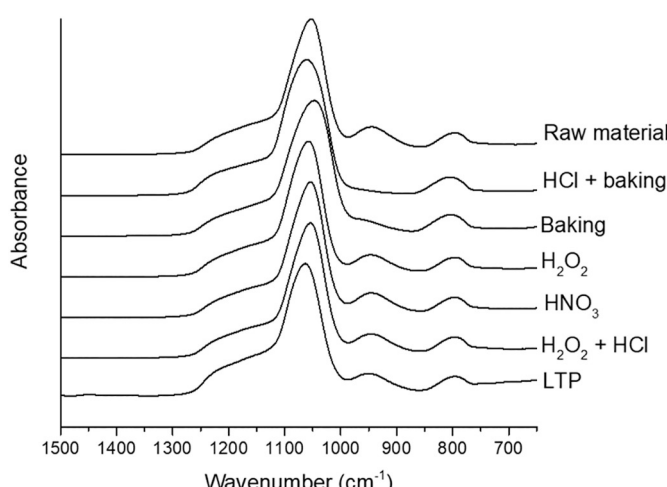


Fig. 3. FT-IR spectra of biogenic silica of *T. pseudonana* before and after cleaning.

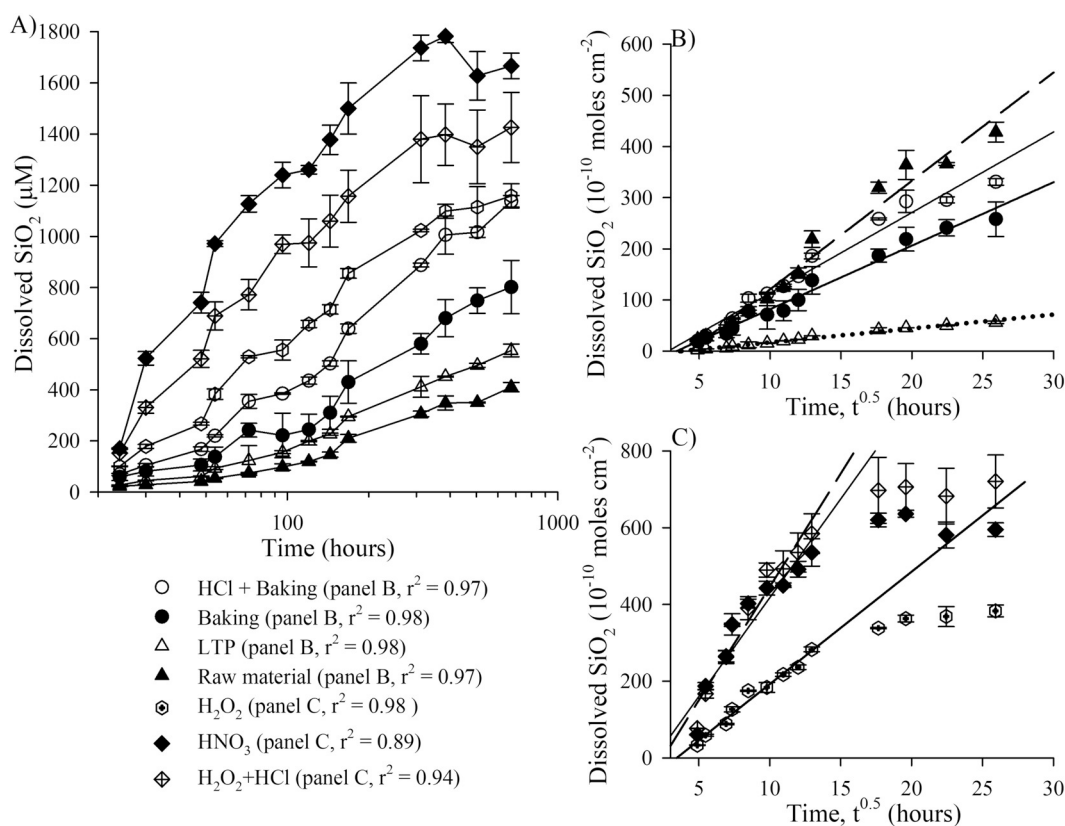


Fig. 4. A) Dissolution profile of *T. pseudonana* biogenic silica in artificial seawater over 672 h (28 days). Error bars are duplicates for each treatment in the measured dissolved SiO_2 . Surface-area (of initial material) normalized dissolved SiO_2 as a function of the square root of time shows parabolic kinetics for the entire time series for HCl + baking, baking only, LTP and raw material (B) or during the initial 168 h (7 days) for H_2O_2 , HNO_3 , and $\text{H}_2\text{O}_2 + \text{HCl}$ (C); error bars are propagated based on uncertainty in dissolved SiO_2 and initial material bSiO₂ per gram (Table 2). Model-I linear regression coefficient of determination (R^2) values are shown in the legend for each treatment over the aforementioned time scales.

(Fig. 6A). However, after ~ 90 days, the total extent of dissolution was the same for both cleaning methods (Fig. 6A). This model system, which was chosen to be more representative of field conditions (i.e. larger diatom, natural seawater matrix), behaved similar to the *T. pseudonana* system when comparing rates (normalized to 28-day $[\text{Si(OH)}_4]$, the longest shared time point among all experiments; Fig. 6A). When examining the normalized rates, the dissolution trends between treatments and diatoms were conserved (Fig. 6B). The dissolution extent/rate in LTP treatments was lower than in HNO_3 treatments for both diatoms with a similar degree of offset between treatments for each organism.

4. Conclusions and recommendations

Samples cleaned with chemical treatments overall exhibited enhanced dissolution rates relative to the LTP treatment (Fig. 5). The consistency in morphology revealed by SEM (Fig. 1) and phase revealed by XRD (Fig. 2) suggests that the increased dissolution rates are not likely due to enhanced porosity of the solid or a change in phase. Lack of variation in morphology and porosity as a function of cleaning method has been previously reported for similar treatment methods (Abramson et al., 2009; Van Eynde et al., 2014).

LTP-treated diatoms have significantly higher surface area than the other treatments, suggesting more efficient removal of organic matter from diatom frustule pores and channels, possibly due to easier access for gas molecules during LTP treatment than of the aqueous phases used for the other treatments. In addition to the initial dissolution rate, the mass recovery associated with LTP was on the higher end among all cleaning treatments and consistently removed $\sim 97\%$ of the total organic matter (Table 2).

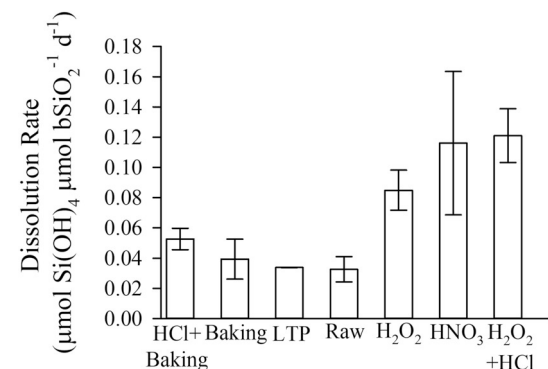


Fig. 5. Average dissolution rate for *T. pseudonana*-derived biogenic silica in artificial seawater. Dissolution rates were determined by fitting a Model-I linear regression to the dissolution profile during the first seven days (nine points) for each treatment, calculating for the mass of SiO_2 based on the container volume, and normalizing to the initial bSiO₂ content in the material (Table 2). Error bars are the standard deviation of duplicates per treatment.

Preparing diatom frustules for use in laboratory-based reactivity experiments should limit the amount of chemical alteration to the frustule. If the process of interest is related to early diagenesis or to simulate remineralization of fresh diatom material in the seabed or water column immediately after bacterial stripping of organic matter, LTP treatment would be recommended. This treatment efficiently removes outer organic matter while not significantly affecting the short- or long-term dissolution of the frustule, especially compared to raw material. This technique was performed in 7 h, which is the least

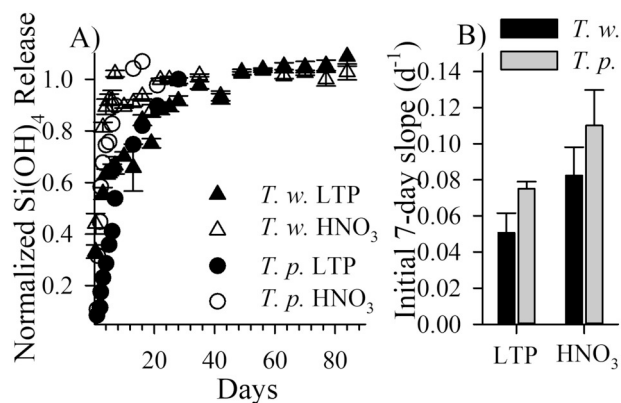


Fig. 6. A) Dissolution profile of *T. weissflogii*-derived biogenic silica in filtered seawater compared to *T. pseudonana* data (Fig. 4); all data was normalized to the silicic acid concentration at the 28-day time point, i.e. the longest time-point shared among all four series. Error \pm standard deviation for triplicate measurements. B) comparison of initial 7-day dissolution slopes for data shown in left panel (based on a logistic expression, hence the units of inverse time), error bar is the standard deviation of the regression fit, where all regressions are statistically significant ($p < .01$) and highly linear ($R^2 = 0.84, 0.87$ for *T. weissflogii* LTP and HNO₃, respectively, and $R^2 = 0.98, 0.82$ for *T. pseudonana* LTP and HNO₃, respectively).

amount of time associated with any of the cleaning methods employed (Table 1). However, if the question of interest is on longer-term time scales, even harsh cleaning methods appear to produce a similar end product and allow for treatment on a quicker experimental time scale with the caveat that some of the harsh methods show a systematic changes in both the three dimensional organization of the SiO₂ framework and the relative abundance of silanol groups. Experiments examining processes occurring after bSiO₂ has dissolved and reached an asymptotic concentration may not have to be as selective in the chemical treatment used for diatom frustules.

Declaration of Competing Interest

The authors declare no competing interests.

Acknowledgements

This work was supported with funding by the National Science Foundation grants OCE-1558957 and 1924585 (JWK), OCE-1559087 and 1923802 (YT), NASA Cooperative Agreement Notice NNN16ZHA001C Experimental Program to Stimulate Competitive Research under contract NNX16AT47A (TGG) and internal support from the Dauphin Island Sea Lab. We also thank S. Acton, L. Cole, W. Dobbins, and I. Marquez for laboratory support.

Appendix A. Supplementary data

Supplementary data to this article can be found online at <https://doi.org/10.1016/j.marchem.2020.103826>.

References

Abramson, L., Wirick, S., Lee, C., Jacobsen, C., Brandes, J.A., 2009. The use of soft X-ray spectromicroscopy to investigate the distribution and composition of organic matter in a diatom frustule and a biomimetic analog. *Deep-Sea Res. II* 56 (18), 1369–1380.

Bidle, K.D., Azam, F., 1999. Accelerated dissolution of diatom silica by marine bacterial assemblages. *Nature* 397 (6719), 508–512.

Bidle, K.D., Brzezinski, M.A., Long, R.A., Jones, J.L., Azam, F., 2003. Diminished efficiency in the oceanic silica pump caused by bacteria-mediated silica dissolution. *Limnol. Oceanogr.* 48 (5), 1855–1868.

Blanco, S., Alvarez, I., Cejudo, C., 2008. A test on different aspects of diatom processing techniques. *J. Appl. Phycol.* 20 (4), 445–450.

Boutorh, J., Moriceau, B., Gallinari, M., Ragueneau, O., Bucciarelli, E., 2016. Effect of trace metal-limited growth on the postmortem dissolution of the marine diatom *Pseudo-nitzschia delicatissima*. *Glob. Biogeochem. Cycles* 30, 57–69.

Boyle, J.A., Pickett-Heaps, J.D., Czarnecki, D.B., 1984. Valve morphogenesis in the pennate diatom *Achnanthes Coarctata*. *J. Phycol.* 20 (4), 563–573.

Dean, W.E., 1974. Determination of carbonate and organic matter in calcareous sediments and sedimentary rocks by loss on ignition - comparison with other methods. *J. Sediment. Petrol.* 44 (1), 242–248.

Demarest, M.S., Brzezinski, M.A., Beucher, C.P., 2009. Fractionation of silicon isotopes during biogenic silica dissolution. *Geochim. Cosmochim. Acta* 73 (19), 5572–5583.

Demarest, M.S., et al., 2011. Net biogenic silica production and nitrate regeneration determine the strength of the silica pump in the eastern equatorial Pacific. *Deep-Sea Research II* 58 (3–4), 462–476.

DeMaster, D., 2003. The diagenesis of biogenic silica: chemical transformations occurring in the water column, seabed, and crust. *Treat. Geochem.* 7, 87–98.

Dixit, S., Van Cappellen, P., 2002. Surface chemistry and reactivity of biogenic silica. *Geochim. Cosmochim. Acta* 66 (14), 2559–2568.

Ellwood, M.J., Hunter, K.A., 2000. The incorporation of zinc and iron into the frustule of the marine diatom *Thalassiosira pseudonana*. *Limnol. Oceanogr.* 45 (7), 1517–1524.

Gendron-Badou, A., Coradin, T., Maquet, J., Frohlich, F., Livage, J., 2003. Spectroscopic characterization of biogenic silica. *J. Non-Cryst. Solids* 316 (2–3), 331–337.

Greenwood, J., Truesdale, V., Rendell, A., 2001. Biogenic silica dissolution in seawater—in vitro chemical kinetics. *Prog. Oceanogr.* 48 (1), 1–23.

Hedges, J.I., Stern, J.H., 1984. Carbon and nitrogen determinations of carbonate-containing solids. *Limnol. Oceanogr.* 29 (3), 657–663.

Hurd, D.C., Birdwhistell, S., 1983. On producing a more general model for biogenic silica dissolution. *Am. J. Sci.* 283 (1), 1–28.

Iler, R.K., 1979. *The Chemistry of Silica*. Wiley- Interscience, New York.

Ingall, E.D., et al., 2013. Role of biogenic silica in the removal of iron from the Antarctic seas. *Nat. Commun.* 4, 1981.

Jeffryes, C., Campbell, J., Li, H., Jiao, J., Rorrer, G., 2011. The potential of diatom nanobiotechnology for applications in solar cells, batteries, and electroluminescent devices. *Energy Environ. Sci.* 4 (10), 3930–3941.

Jiang, W., et al., 2014. Purification of biosilica from living diatoms by a two-step acid cleaning and baking method. *J. Appl. Phycol.* 26 (3), 1511–1518.

Kamatani, A., Riley, J.P., Skirrow, G., 1980. The dissolution of opaline silica of diatom tests in sea water. *J. Oceanogr. Soc. Jpn.* 36 (4), 201–208.

Kamatani, A., Ejiri, N., Treguer, P., 1988. The dissolution kinetics of diatom ooze from the Antarctic area. *Deep-Sea Res.* 35 (7), 1195–1203.

Kester, D.R., Duedall, I.W., Connors, D.N., Pytkowic, R., 1967. Preparation of artificial seawater. *Limnol. Oceanogr.* 12 (1), 176–179.

Koning, E., Gehlen, M., Flank, A.M., Calas, G., Epping, E., 2007. Rapid post-mortem incorporation of aluminum in diatom frustules: evidence from chemical and structural analyses. *Mar. Chem.* 106 (1–2), 208–222.

Krause, J.W., et al., 2010. The effects of biogenic silica detritus, zooplankton grazing, and diatom size structure on silicon cycling in the euphotic zone of the eastern equatorial Pacific. *Limnol. Oceanogr.* 55 (6), 2608–2622.

Krause, J.W., et al., 2017. Reactive silica fractions in coastal lagoon sediments from the northern Gulf of Mexico. *Cont. Shelf Res.* 151, 8–14.

Krausse, G.L., Schelske, C.L., Davis, C.O., 1983. Comparison of three wet-alkaline methods of digestion of biogenic silica in water. *Freshw. Biol.* 13, 73–81.

Laruelle, G.G., et al., 2009. Anthropogenic perturbations of the silicon cycle at the global scale: key role of the land-ocean transition. *Glob. Biogeochem. Cycles* 23.

Lawson, D.S., Hurd, D.C., Pankratz, H.S., 1978. Silica dissolution rates of decomposing phytoplankton assemblages at various temperatures. *Am. J. Sci.* 278 (10), 1373–1393.

Legrand, A.P., 1998. *The Surface Properties of Silica*. Wiley, New York.

Lewin, J.C., 1961. The dissolution of silica from diatom walls. *Geochim. Cosmochim. Acta* 21 (3–4), 182–198.

Losic, D., Mitchell, J.G., Voelcker, N.H., 2009. Diatomaceous lessons in nanotechnology and advanced materials. *Adv. Mater.* 21 (29), 2947–2958.

Loucaides, S., Behrends, T., Van Cappellen, P., 2010a. Reactivity of biogenic silica: surface versus bulk charge density. *Geochim. Cosmochim. Acta* 74 (2), 517–530.

Loucaides, S., et al., 2010b. Seawater-mediated interactions between diatomaceous silica and terrigenous sediments: results from long-term incubation experiments. *Chem. Geol.* 270 (1), 68–79.

McManus, J., et al., 1995. Early diagenesis of biogenic opal - dissolution rates, kinetics, and paleoceanographic implications. *Deep-Sea Res. II* 42 (2–3), 871–903.

Michalopoulos, P., Aller, R.C., 1995. Rapid clay mineral formation in Amazon delta sediments: reverse weathering and oceanic elemental cycles. *Science* 614.

Michalopoulos, P., Aller, R.C., Reeder, R.J., 2000. Conversion of diatoms to clays during early diagenesis in tropical, continental shelf muds. *Geology* 28 (12), 1095–1098.

Morales, L.V., Sigman, D.M., Horn, M.G., Robinson, R.S., 2013. Cleaning methods for the isotopic determination of diatom-bound nitrogen in non-fossil diatom frustules. *Limnol. Oceanogr. Meth.* 11, 101–112.

Rahman, S., Aller, R.C., Cochran, J.K., 2017. The missing silica sink: revisiting the marine sedimentary Si cycle using cosmogenic ³²Si. *Glob. Biogeochem. Cycles* 31 (10), 1559–1578.

Schmidt, M., et al., 2001. Oxygen isotopes of marine diatoms and relations to opal-a maturation. *Geochim. Cosmochim. Acta* 65 (2), 201–211.

Strickland, J.D., Parsons, T.R., 1972. *A Practical Handbook of Seawater Analysis*.

Stumm, W., Morgan, J.J., 1996. *Aquatic Chemistry: Chemical Equilibria and Rates in Natural Waters*. Wiley, New York (1022 pp).

Tesson, B., et al., 2008. Contribution of multi-nuclear solid state NMR to the characterization of the *Thalassiosira pseudonana* diatom cell wall. *Anal. Bioanal. Chem.* 390 (7), 1889–1898.

Tréguer, P.J., De La Rocha, C.L., 2013. The World Ocean silica cycle, annual review of marine science, Vol 5. *Annu. Rev. Mar. Sci.* 477–501.

Tyler, J.J., Leng, M.J., Sloane, H.J., 2007. The effects of organic removal treatment on the integrity of delta(18)O measurements from biogenic silica. *J. Paleolimnol.* 37 (4), 491–497.

Van Cappellen, P., Dixit, S., van Beusekom, J., 2002. Biogenic silica dissolution in the oceans: reconciling experimental and field-based dissolution rates. *Glob. Biogeochem. Cycles* 16 (4).

Van der Werff, A., 1955. A new method of concentrating and purifying diatoms and other organisms. *Fundamental Appl. Limnol.* 12, 276–277.

Van Eynde, E., et al., 2014. Effect of pretreatment and temperature on the properties of *Pinnularia* biosilica frustules. *RSC Adv.* 4 (99), 56200–56206.

Watanabe, T., Kodama, Y., Mayama, S., 2010. Application of a novel cleaning method using low-temperature plasma on tidal flat diatoms with heterovalv or delicate frustule structure. *Proc. Acad. Natl. Sci. Phila.* 160 (1), 83–87.

Xiong, Z.F., Li, T.G., Crosta, X., 2012. Cleaning of marine sediment samples for large diatom stable isotope analysis. *J. Earth Sci.* 23 (2), 161–172.

Zhuravlev, L.T., 2000. The surface chemistry of amorphous silica. Zhuravlev model. *Colloids Surf. A Physicochem. Eng. Aspects* 173 (1–3), 1–38.